Thermochimica Acta 513 (2011) 9–19

Contents lists available at ScienceDirect

Thermochimica Acta

journal homepage: www.elsevier.com/locate/tca

Comparison of analytic and numerical solutions for a burning soot bed in confined walls

Chunsung Lee[a], Byunghwa Lee[a], Gyubo Kim[b], Chunghwan Jeon[c], Youngjune Chang[c], Juhun Song[c,*]

[a] Graduate Program, School of Mechanical Engineering, Pusan National University, Republic of Korea
[b] Pusan Clean Coal Center, Republic of Korea
[c] School of Mechanical Engineering, Pusan National University, Pusan Clean Coal Center, San 30, Jangjeon-dong, Geumjeong-gu, Busan, Republic of Korea

ARTICLE INFO

Article history:
Received 11 August 2010
Received in revised form 9 October 2010
Accepted 20 October 2010
Available online 3 November 2010

Keywords:
Numerical solution
Combustion
Soot bed
Confined wall
Advection

ABSTRACT

A one-dimensional model that describes diffusion and advection process has been developed. The approximate solution to the nonlinear equations has been obtained analytically with an iterative method. A two-dimensional numerical solution with computational fluid dynamics (CFD) software is also derived for a two-dimensional crucible around which the convective and diffusive flows are more precisely presented. The results showed that as long as both heat and oxygen diffusion processes are considered at a time, the one-dimensional solution could provide as accurate a result as that obtained by using the two-dimensional solution evaluated in terms of temperature, but not in terms of the oxygen content. The weight and the geometry of the soot bed significantly affect the distribution of temperature and oxygen content that warrants the use of two-dimensional model because a two-dimensional character such as a buoyant upward flow from the relatively hot bed is predominant.

1. Introduction

In order to describe the rate-controlling combustion processes of a soot bed burning in a confined crucible of TGA, a number of analytical models and solutions have been documented in the literatures for a transfer of heat and mass along the surface of soot bed. However, most of the models have been limited to a separate consideration of either diffusion process since a complete coupling of heat transfer with mass transfer leads to a nonlinear system of equations requiring a relatively complicated solution method. As an example, some researchers have developed a mathematical model to obtain the oxygen distribution along the soot bed; it is essential to know this distribution in order to determine the intrinsic reactivity of soot combustion. However, the temperature gradients within a particle were not addressed simultaneously although these gradients could alter the combustion rate as significantly as the gradient of the oxygen concentration [1–4]. In particular, Stanmore et al. [4] evaluated the mean transfer coefficient (h_m) of oxygen to the bed surface; the value of this coefficient is required in their one-dimensional analysis for a thermobalance with a vertical flow by simply considering the crucible in the furnace as the upstream side of a symmetrical bluff body. The knowledge of the drag (or friction) coefficient could give the mean mass transfer coefficient using the Reynolds analogy of boundary layers under the Stokes flow regime with low Reynolds number [5].

In other literatures [6,7], a two-dimensional numerical simulation has been employed for a thermobalance with a horizontal flow in order to demonstrate the significant difference in the oxygen concentration over a soot bed, indicating the importance of the effect of the oxygen concentration on the combustion of the soot bed burning under a TGA condition. In the simulation study of Marcuccilli et al. [6], a two-dimensional mathematical model of oxygen transfer was developed to extract the true kinetic rates because significant oxygen depletion occurred along both directions because of the transverse fluid motion across the lip of the crucible. Furthermore, the concentration boundary layer of oxygen could not fully develop above the bed, thereby necessitating a two-dimensional approach. However, the external flow from the crucible top to the bed surface was considered to be uniform, and the real nature of the hydrodynamic flow that develops around the crucible was not considered in their model. As a result, the presence of a crucible wall affecting the boundary layer conditions and the subsequent transfers of oxygen and heat were not simultaneously accounted for in the model. In a more refined analysis for the same TGA system [7], a more precise consideration of the real external flow and bed configurations in the CFD code allowed the corrected computation of the mean mass transfer coefficient of oxygen, which is again essential for determining the true kinetics. The coefficient was found to be strongly dependent on the presence of the front and the rear walls of the crucible and the deposition of the soot bed. However, in order

* Corresponding author. Tel.: +82 51 510 7330; fax: +82 51 512 5236.
E-mail address: jxs704@pusan.ac.kr (J. Song).

0040-6031/$ – see front matter © 2010 Elsevier B.V. All rights reserved.
doi:10.1016/j.tca.2010.10.011

Nomenclature

A	frequency factor
A_c	cross-sectional area of TGA crucible
C	molar concentration
$C_{p,\,gmol}$	molar heat capacity
D_e	molar external diffusivity
D_b	molar bed diffusivity
k	intrinsic rate constant
E_a	activation energy
B_f	heat blowing factor [unitless]
B_m	mass blowing factor [unitless]
L_s	height of soot bed
L_∞	height of TGA crucible at ambient conditions
T	temperature
r_c	carbon consumption rate [g/s]
r_{O_2}	oxygen consumption rate [mol/s]
$\dot{n}$	molar flow rate of oxygen
$\dot{q}$	heat flow rate
x	distance from a crucible bottom to a point inside soot bed
x_{O_2}	oxygen mole fraction [dimensionless]
MW_c	molecular weight of carbon
Δh_c	heat of carbon reaction
R_u	universal gas constant
Re	Reynolds number
Gr	Grashof number

Greek characters

λ	thermal conductivity
ρ	density
ε	porosity
ψ	CO_2 fraction in a product gas
ϕ_t	Thiele diffusion modulus for heat transfer within soot bed
ϕ_m	Thiele diffusion modulus for mass transfer within soot bed
α	thermal diffusivity, $\alpha = \lambda/\rho C_p$

Subscripts

g	gas phase
b	bed phase (solid)
c	carbon or crucible
O_2	oxygen
s	top surface of soot bed
o	bottom surface of soot bed, at location $x = 0$
∞	ambient bulk flow condition
e	external clearance above soot bed in TGA crucible
$'''$	volumetric based (heat or molar flow rate)
h	homogeneous solution
p	particular solution
t	total flow rate

to obtain the coefficient, a nonreacting flow is modeled in the CFD code under an isothermal condition where the temperature gradient produced by the exothermicity of the soot reaction and ensuing natural convection were assumed to be negligible with respect to their effect on the mass transfer for each particular condition.

There is another work of Liang and Kozinski [8] on the modeling of the combustion and pyrolysis of the solid bed in the TGA although this may be more related to the combustion of cellulosic biomass. A numerical model was developed in which the effect of the convective and the diffusive flows was not considered while the heat conduction over the crucible was considered to be the primary transport to the particle surface. Moulijn et al. have developed a numerical model that qualitatively describes the heat and oxygen transport within a crucible and their influence on the combustion rate [9]. Despite these prior researches, there is yet a need to develop simple one-dimensional models that describe the local gradients of both the temperature and the oxygen in the gas and the bed phases. These models should then be validated against a more accurate solution from two-dimensional numerical models, which are believed to be a more precise representation of the convective and diffusive flows around the crucible.

In this study, a new model that considers both the transport processes that occur above and within a soot bed is developed. In this model, the gas phase and in-bed transfer processes have been coupled, which is relatively simple yet accurate. The resultant set of nonlinear equations is solved with the Newton–Raphson iterative method in order to calculate the temperature and the oxygen content along the surface of the soot bed. During the analysis, several dimensional parameters were evaluated in order to determine their relative importance in response to changes in ambient gas temperatures. The validity and limitation of this one-dimensional analytic technique were evaluated particularly for the soot bed with a variety of geometries in confined walls that might be encountered in more real applications.

2. Modeling and solution methods

2.1. One-dimensional model

Fig. 1 presents the dimensional geometry of the soot bed and the crucible used for this analytic computation where the anticipated profiles are plotted for temperature and oxygen concentrations against the stream wise direction, which is considered to be one dimension. The temperature and the concentration were assumed to remain constant along the direction normal to the flow direction, which should be validated by comparing with the two-dimensional result. As described in Section 1, most of the one-dimensional analytical models documented in the literature are characterized by a biased consideration of either one of the two diffusion processes of heat and mass. Because of the uncoupling of two diffusions, these models failed to describe the exact aspect of the combustion processes for a burning soot bed in the confined walls of crucible used for TGA, where a transfer of heat and mass along the surface of the soot bed are involved in a coupled manner. Nonetheless, these models have been widely used for a certain condition where one of two transfers is neglected under an isothermal or constant concentration condition: if the gradient of either the temperature or the species concentration is low, the heat and the mass transfers will not occur concurrently. Accordingly, one of these diffusion models is separately selected. Such a model commonly leads to a straightforward equation and provides its solution without extensive computational efforts. For example, under a known thermal condition (whether it is assumed to be constant or determined through a calculation), the influence of the oxygen diffusion process was separately analyzed with a simplified modeling of oxygen transfer exclusively through three different diffusion processes [1–3] During this analysis, the influence of the advective flow on both the transfers is further assumed to be negligible because the flow around the crucible is known to be in the Stokes flow regime where the flow rate (velocity) of the bulk flow and the crucible size are relatively small [1]. Furthermore, the mass diffusional transfer is only limited to the reactant gas of oxygen; it did not extend to the product gases of CO or CO_2. In contrast, an integrated model combining the diffusive processes mentioned above and within the soot bed at a certain time is developed here. The model is analytically solved to predict four variables such as temperatures and

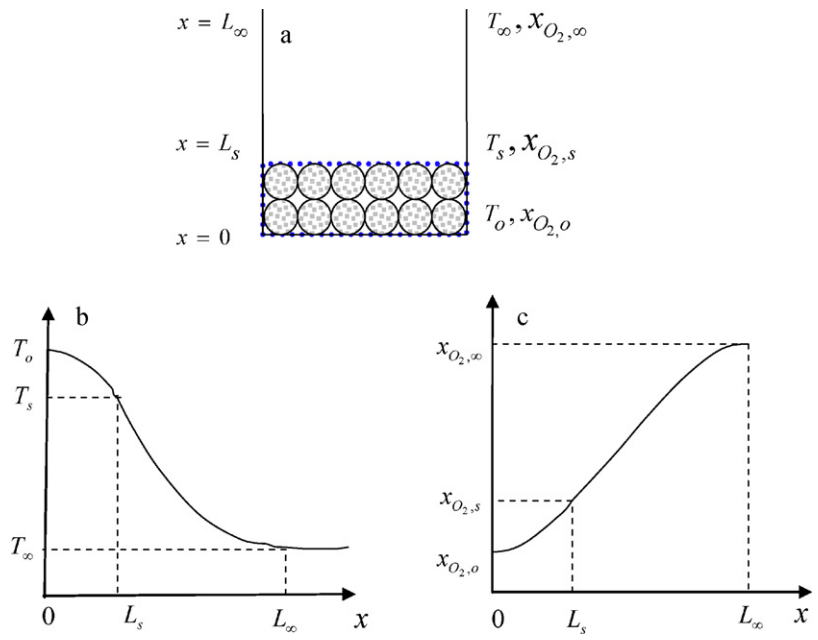

Fig. 1. (a) One-dimensional schematic representation of soot bed and crucible used for the one-dimensional method, and anticipated profiles of (b) gas temperature and (c) oxygen concentration.

oxygen contents at two surfaces of the soot bed. These are eventually used for providing the distribution of temperatures and oxygen contents beyond and within the soot bed, as discussed in the next subsections.

2.1.1. Energy balance at a bed surface

The principle of the surface energy balance ($\dot{E}_{in} = \dot{Q}_{out}$) was employed at the top surface of the soot bed where the convective transfer rate at the surface is equal to the rate of heat release from the soot bed. In order to obtain the right-hand term, that is, the outgoing energy or convective transfer rate ($\dot{Q}_{out}$), it is essential to know the temperature distribution of the gas from an ambient bulk flow to the top surface of the soot bed. This requires the solution of a second-order ordinary differential equation with appropriate boundary conditions where the heat diffusion and the advection effects are included in a gas phase for the energy balance over its infinitesimal control volume (although the full derivation is not shown in detail here).

$$\dot{Q}_{out} = \frac{A_C \cdot \lambda_g}{(L_S - L_\infty)} \cdot \frac{B_f \cdot e^{Bf}}{1 - e^{Bf}} \cdot (T_S - T_\infty) \tag{1}$$

The left-hand term, incoming energy, is the same as the heat release of the soot bed due to the volumetric reaction evaluated under the condition of a constant oxygen concentration along the bed.

$$\dot{E}_{in} = \dot{q}''' \cdot A_C \cdot L_S = (k \cdot \rho_b \cdot x_{O_2,S} \cdot C \cdot R_u \cdot T_s \cdot \Delta h_c) \cdot A_c \cdot L_s \tag{2}$$

Equating both terms gives rise to Eq. (3) given below, as expressed in terms of two variables. In this equation, it is apparent that the temperature at the top of the particle layer (T_s) and $x_{O_2,S}$ are unknown and to be solved while the other parameters such as ambient temperature (T_∞) are known and treated as constants.

$$f_1(T_S, x_{O_2,S}) = k \cdot \rho_b \cdot x_{O_2,S} \cdot C \cdot R_u \cdot T_s \cdot \Delta h \cdot L_S - \frac{\lambda_g}{(L_S - L_\infty)} \cdot \frac{B_f \cdot e^{Bf}}{1 - e^{Bf}} \cdot (T_S - T_\infty) = 0 \tag{3}$$

where k is the intrinsic rate constant that is expressed in an Arrhenius form for exhibiting a temperature dependence ($= A \exp(-E_a/R_u \cdot T_s)$). B_f is the heat blowing factor that is a dimensionless parameter as defined in

$$B_f = \frac{(1 - \psi) \cdot C_{p,mol} \cdot [k \cdot \rho_b \cdot x_{O_2,S} \cdot C \cdot R_u \cdot T_s \cdot L_s] \cdot (L_s - L_\infty)}{2 \cdot \lambda_g \cdot MW_C}$$

Introduced for the sake of computational simplicity, the heat blowing factor is a dimensionless parameter that is analogous in form to the Damkoler number widely used in flame study. In the definition of the blowing factor, the numerator is a heat generation that is strongly affected by the heat storage capacity of the soot bed and the consumption rate of the soot bed, while the denominator is the heat loss related to the thermal conductivity of the soot bed. Therefore, it could provide a measure of how much more importantly is the heat source involved than the heat loss. Provided that the heat loss effect from the conduction is lesser than the heat source effect transferred by the advection induced from the reaction of the soot bed, the factor is expected to increase, thereby resulting in the presence of a steeper temperature gradient between the top surface of the soot bed and the crucible top.

2.1.2. Oxygen balance at a bed surface

As previously done for the energy, the mole balance of the oxygen species ($\dot{n}_{O_2,in} = \dot{n}_{O_2,out}$) was applied at the top surface of the soot bed with notable opposition in the direction of the oxygen species flux. The outgoing mass flow is the same as the oxygen consumption rate occurring over the entire volume of the soot bed:

$$\dot{n}_{out} = r'''_{O_2} \cdot A_C \cdot L_S = -\frac{(1 + \psi) \cdot k \cdot \rho_b \cdot (x_{O_2,S} \cdot C \cdot R_u \cdot T_s) \cdot [A_s \cdot L_s]}{2MW_C} \tag{4}$$

The incoming mass flow is due to the fluid motion of the gases from the molecular diffusion and advection, $\dot{n}_{in} = (A_C \cdot \wp_e \cdot C/(L_S - L_\infty)) \cdot [B_m \cdot e^{Bm}/(1 - e^{Bm})] \cdot (x_{O_2,S} - x_{O_2,\infty})$. By recognizing both flux terms for the oxygen balance, we can derive the following expres-

sion in Eq. (5) expressed in terms of the two primary variables:

$$f_2(T_S, x_{O_2,S}) = \frac{(1+\psi)\cdot k\cdot \rho_b \cdot x_{O_2,S}\cdot R_u \cdot T_s \cdot L_s}{2MW_C} + \frac{\wp_e}{(L_S - L_\infty)} \cdot \left[\frac{B_m \cdot e^{Bm}}{1-e^{Bm}}\right]\cdot (x_{O_2,S} - x_{O_2,\infty}) = 0 \quad (5)$$

where B_m is the mass blowing factor that is a dimensionless parameter as defined in

$$B_m = \frac{(1-\psi)\cdot[k\cdot\rho_b\cdot x_{O_2,S}\cdot C\cdot R_u\cdot T_s\cdot L_s]}{2\cdot\wp_e\cdot C\cdot MW_C}\cdot(L_s - L_\infty)$$

Similar to the heat blowing factor, this factor is a dimensionless parameter that is a type of the external Thiele modulus although it does not include the reaction rate of the gases but includes the reaction rate of the soot bed. Since this factor is the ratio of reaction rate of the soot bed to the diffusivity of the gases, it can provide a measure of how much reaction is involved than a molecular diffusion to consume the oxygen available. Therefore, an increase in this factor can result in the presence of a relatively high oxygen consumption at the top surface of the soot bed and thereby a relatively steep gradient of the oxygen concentration between the top surface of the soot bed and the crucible top.

2.1.3. Energy balance inside the soot bed

The primary purpose of this energy balance is to provide the third equation where the temperature at the bottom surface of the particle layer (T_o) is related with other parameters and variables. This can be attained by employing an energy balance over a finite control volume enclosing the soot bed. There are several different approaches in the literature that depend on how accurately the combustion rate and its corresponding heat generation are modeled within the soot bed. The simplest method is to assume the heat release rate ($\dot{q}'''$) on a volume basis to be constant and uniformly distributed over the bed, which greatly eliminates the appearance of a nonlinear exponential function of temperature in the energy balance equation within the soot bed [3]. In contrast to the abovementioned approach, the present approach considers $\dot{q}'''$ to be non-uniform and varied over the bed. With this assumption, the energy balance can be applied for the control volume of the soot bed: $q_x - q_{x+dx} + \dot{q}''' \cdot A_C\, dx = 0$ where molecular heat diffusion and reaction are involved. Within the bed, there exists heat diffusion and heat generation containing the combustion rate, which strongly depends on the temperature. The advection effect is neglected for the heat transfer flux at the two faces of the control volume, which may be due to the considerably lower velocity than that of gas above the soot bed with its one side closed. It is apparent that because of the appearance of the exponential terms on the right side, the resultant equation (see below) is nonlinear in terms of temperature; this necessitates a further linearization. It should also be noted that there is another model in which the reaction and the advection are included within the soot bed with one side open under the negligence of conduction [10].

$$\frac{d^2T}{dx^2} = -\frac{\rho_b\cdot CO_2\cdot R_u\cdot \Delta h_c}{\lambda_S}\cdot k(T)\cdot T \quad (6)$$

By using $e^{-x} \approx 1 - x$ at small x, we can approximate the rate constant into a linearized term of $k(T) \approx A\cdot[1 - E_a/R_u\cdot T]$. After this term is included, the equation is rearranged as

$$\frac{d^2T}{dx^2} + \frac{\rho_b\cdot CO_2\cdot R_u\cdot \Delta h_c\cdot A}{\lambda_b}\cdot T = \frac{\rho_b\cdot CO_2\cdot R_u\cdot h_c\cdot A}{\lambda_b}\cdot\frac{E_a}{R_u} \quad (7)$$

By solving the Eq. (7) with the two boundary conditions, $dT/dx|_{X=0} = 0$ and $T|_{X=L\cdot S} = T_S$, we find the homogeneous solution to be a trigonometric function of x, the distance from the crucible bottom to a point inside the soot bed. By combining this solution with the non-homogeneous solution, we can obtain the total solution as

$$T(x) = T_h + T_P = \frac{T_S}{\cos\phi_t}\cdot\cos\left(\phi_t\cdot\frac{x}{L_S}\right) + \frac{E_a}{R_u} \quad (8)$$

where ϕ_t is the thermal Thiele modulus that represents the ratios of the heat generated within the soot bed over the thermal condition. This modulus is expressed as

$$\phi_t = L_S\cdot\sqrt{\frac{\rho_b\cdot x_{O_2}\cdot C\cdot R_u\cdot\Delta h_c\cdot A}{\lambda_b}}$$

From the above temperature profile along the soot bed, we can eventually obtain the relation (Eq. (9)) for the temperature at the bottom surface by calculating $T|_{x=0}$.

$$f_3(T_O, T_S, x_{O_2,S}, x_{O_2,O}) = T_O - \frac{T_S}{\cos\phi_t} - \frac{E_a}{R_u} = 0 \quad (9)$$

2.1.4. Oxygen balance inside the soot bed

In order to close the set of equations with the four variables described earlier, one additional equation is required. Over the control volume used in energy balance, the net transfer of oxygen species at the surface from the molecular diffusion are balanced with the oxygen depletion from the reaction within the control volume; $q_x - q_{x+dx} - r'''_{O_2}\cdot A_C\, dx = 0$. In a manner similar to the energy balance, the transport of oxygen from advection is assumed to be negligible, while a volumetric oxygen depletion is based on the oxygen mole that depends linearly on the oxygen concentration. The resultant equation becomes

$$\frac{d^2x_{O_2}}{dx^2} - \frac{(1+\psi)\cdot k\cdot\rho_b\cdot R_u\cdot T}{2MW_C\cdot\wp_b}\cdot x_{O_2} = 0 \quad (10)$$

By solving the equation with the two boundary conditions, $dx_{O_2}/dx|_{x=0} = 0$ and $x_{O_2}|_{x=L_S} = x_{O_2,S}$, we find the total solution to be a hyperbolic function of x, the distance from the crucible bottom to a point inside the soot bed of the TGA.

$$x_{O_2} = \frac{x_{O_2,S}}{\cosh\phi_m}\cdot\cosh\left(\phi_m\cdot\frac{x}{L_S}\right) \quad (11)$$

where ϕ_m is the Thiele modulus within the soot bed, which represents the ratios of reaction resistance over the diffusional resistance and is expressed as

$$\phi_m = L_S\cdot\sqrt{\frac{(1+\psi)\cdot A\,\exp(-E_a/R_uT)\cdot\rho_b\cdot R_u\cdot T}{2MW_C\cdot\wp_b}}$$

From the above profile of oxygen fraction along the soot bed, the Eq. (12) relating oxygen concentration at the bottom surface with other variables is eventually obtained by calculating $x_{O_2}|_{x=0} (= x_{O_2,O})$

$$f_4 = f_n(T_S, T_o, x_{O_2,o}, x_{O_2,S}) = x_{O_2,o} - \frac{x_{O_2,S}}{\cosh\phi_m} = 0 \quad (12)$$

Through these derivations, a complete coupling of the heat transfer with the mass transfer is possible, yielding a nonlinear system of Eqs. (1)–(4) that requires a relatively complicated solution technique. The set of nonlinear equations was solved with an iterative method to calculate four variables such as temperatures and oxygen contents at the two surfaces of the soot bed. In order to solve this set of equations, we required the kinetic rate parameters for a solid reaction that occurs within the soot bed, as listed in Table 1. The values were found to fall into the ranges between the maximum and the minimum values available in the literature. In addition, the relations of the thermodynamic and transport properties of the soot bed and the reacting gases are listed in Table 2, while other properties are found in Nomenclature. Most of the properties used in

the equation are taken from the literatures on coal char combustion [11,12] and soot combustion [13]. It should be noted that the temperature variation is considered for specific properties such as heat capacity and thermal conductivity.

2.2. Two-dimensional model

A commercial CFD package such as FLUENT was used for providing a two-dimensional solution that would be a more precise representation of the advective and the diffusive flows around the crucible.

2.2.1. Gaseous flow

In the case of gas phase flow around and within the crucible, it is obvious that the mass transfer model is coupled with the heat and momentum transfer models, which are already incorporated in a set of governing equations available in the software.

Momentum equation:

$$\frac{\partial}{\partial t}(\rho\vec{v}) + \nabla\cdot(\rho\vec{v}\vec{v}) = -\nabla p + \nabla\cdot(\bar{\bar{\tau}}) + \rho\vec{g} \quad (13)$$

where p is the static pressure, $\bar{\bar{\tau}}$ is the stress tensor, and $\rho\vec{g}$ is the gravitational body force. The momentum diffusion due to the viscous force is considered in the momentum balance equation in addition to the inertia force from the advection as well as a gravity-driven body force.

Table 1
Kinetic rate parameters used for reaction of soot bed in analytic and numerical methods.

Parameters	Values
Activation energy, E_a	102.3 [kJ/mol]
Frequency factor, A	0.044 [1/Pa s]

Energy equation:

$$\frac{\partial}{\partial t}(\rho E) + \nabla\cdot(\vec{v}(\rho E + p)) = \nabla\cdot\left(k_{eff}\nabla T - \sum_j h_j\vec{j}_j + (\overline{\overline{\tau_{eff}}}\cdot\vec{v})\right) \quad (14)$$

where $E = h + \vec{v}^2/2$. The sensible enthalpy h is defined for ideal gases, k_{eff} is the effective conductivity, and $\vec{j}_j$ is the diffusion flux of species j. The terms on the right-hand side represent the energy transfer due to conduction, species diffusion, and viscous dissipation, respectively.

Species equation:

$$\frac{\partial}{\partial t}(\rho Y_i) + \nabla\cdot(\rho\vec{v}Y_i) = -\nabla\cdot\vec{j}_i \quad (15)$$

where Y_i is the local mass fraction of each species through the solution of a convection–diffusion equation for the ith species; $\vec{j}_i$ is the diffusion flux of the species.

As shown in the three equations, advection and molecular laminar diffusion were the two primary processes for all transfers. It

Table 2
Thermodynamic and transport property relations of gas and soot bed used for the one-dimensional analysis.

Phases	Properties	Empirical relations	Unit
Gas	Thermal conductivity λ_g	$\left[(10.4\times10^{-5}) + (5.56\times10^{-7})\times\left(\frac{T_s+T_\infty}{2}\right)\right]$	J/s cm K
	Molar heat capacity $C_{p,\,gmol}$	$\left\{\frac{[\psi\times(0.92+0.00047^{T_\infty})\times44]}{10^3}\right\} + \left\{\left[\frac{(1-\psi)\times(0.92+0.00047^{T_\infty})\times28}{10^3}\right]\right\}$	J/mol K
	Molar external diffusivity D_e	$\left(\frac{0.5\times(T_s+T_\infty)}{T_{ref}}\right)^{1.5}\times D_{ref}$, $D_{ref} = 0.16$	cm²/s
Soot bed	Bed diffusivity D_b	$D_e\cdot\frac{\varepsilon_b}{\tau_b}$	cm²/s
	Density ρ_b	Constant (1.5)	g/cm³
	Porosity ε_b	Constant (0.5)	Unitless
	Tortuosity τ_b	Constant (2.1)	Unitless
	Carbon thermal conductivity λ_c	Constant (2.5×10^{-3})	J/s cm K
	Bed thermal conductivity λ_b	$=\varepsilon_b\lambda_g + (1-\varepsilon_b)\lambda_c$	J/s cm K
	Heat of reaction Δh_c	$=\frac{[26.4(1-\psi)+94.1\psi]\times4.18\times1000}{12}$	J/g

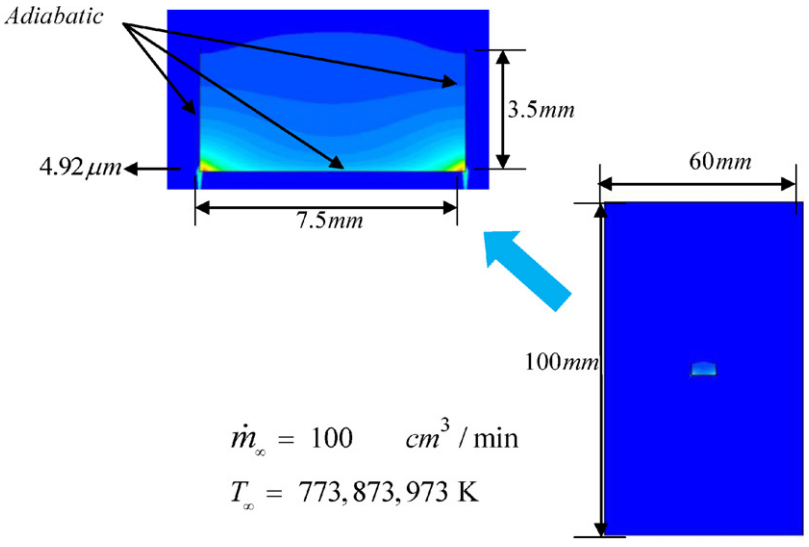

Fig. 2. Geometrical details of the crucible and furnace used for two-dimensional numerical method where inlet conditions at the furnace and boundary conditions at the crucible wall are prescribed.

should be noted that neither the turbulence model nor the reaction model is included. At the three-sided wall of the crucible, adiabatic, non-slip and impermeable conditions are prescribed as the boundary conditions. The velocity and temperatures calculated from the volume flow rate (100 cm^3/min) and furnace diameter (60 mm) are given at the furnace inlet for the ambient flow around the crucible, while the outflow condition is pertinent to the outlet of the furnace. The geometrical details of the crucible and the heated furnace are described with the inlet conditions and boundary conditions in Fig. 2.

2.2.2. Reacting soot bed

There is a simple treatment of the reaction of soot bed in the literature, including the numerical work of Lecomte et al. [14], where a heat source in a gaseous volume is considered simply for an original soot-bed region. Within this area, the constant rate of the volumetric heat generation is distributed uniformly. However, the lack of oxygen depletion and its resultant motion of product gases in the numerical models could readily underpredict the oxygen concentration along the crucible during the soot bed reaction. In this two-dimensional approach, the reaction model of the soot bed in a solid phase was considered to be a relatively hot oxygen-depleting source, which could thus induce the advection of a buoyant flow as well as the molecular diffusion of oxygen. The reaction is typically assumed to be a global reaction with a single step where the reaction rate is linearly proportional to the oxygen concentration. It is necessary to convert the rate constant expressed for a solid reaction to that for the oxygen in the gas phase, which is expressed in terms of moles. In particular, the soot bed is approximated as a porous fixed bed where the simple reaction of $C + (1+\psi)/2\, O_2 \rightarrow (1-\psi)CO + \psi CO_2$ occurs in the bed that is penetrated by both oxygen and the product gases. Thus, both mass and heat production from a reacting bed would be included in the following two conservation equations when the advection transfer from a fluid motion was absent.

Species equation:

$$-\nabla \cdot \vec{j}_i + \frac{dm_i}{dt} = 0 \tag{16}$$

where $\vec{j}_i$ is the diffusion flux of species i and dm_i/dt is the net rate of depletion of species i by the chemical reaction at the particle surface (kg/s). This rate of depletion is given as:

$$\frac{dm_j}{dt} = A_b Y_j R_j = A_b Y_j R_{kin} \left(p_n - \frac{R_j}{D_0} \right)^n \tag{17}$$

where A_b is the surface area of the soot bed (m^2), Y_j is the mass fraction of the surface species j in the particle, p_n is the bulk pressure of the gas phase species (Pa), D_0 is the diffusion rate coefficient, R_{kin} is the kinetic rate of reaction ($= AT_p e^{-(E/RT_p)}$), and n is the apparent order of reaction.

Energy equation:

$$\nabla \cdot \left(k_{eff} \nabla T - \sum_j h_j \vec{j}_j \right) + S_h = 0 \tag{18}$$

where k_{eff} is the effective conductivity, $\vec{j}_j$ is the diffusion flux of species j, and S_h includes the heat release of the chemical reaction ($= (dm_p/dt) \cdot \Delta h_c = [dm_j/dt \cdot 2/(1+\Psi) \cdot MW_c] \cdot \Delta h_c$).

The two terms in the bracket of the energy equation represent the energy transfer due to conduction and the species diffusion, respectively. The same kinetic rate parameters used for the one-dimensional simulation were employed in this simulation. Further, the temperature-dependent properties of the gas and the soot bed available in the FLUENT are reconfirmed to be in the same order of magnitude as those for the one-dimensional simulation listed in Table 2.

Table 3
Results of temperatures and oxygen mole fractions at two surfaces of soot bed computed using one-dimensional analytic method.

Ambient gas temperatures (K)	T_s (K)	T_o (K)	$x_{O_2,s}$	$x_{O_2,o}$
773	776.8	776.8	0.2091	0.2091
873	896.3	896.3	0.2050	0.2050
973	1072.2	1072.2	0.1899	0.1899

3. Calculation results

3.1. Analytical solution results

The computed temperatures and oxygen concentrations derived from the one-dimensional analytic method are listed on the two sides of a particle layer (i.e., $x = 0$ and $x = L_s$) for three different ambient gas temperatures in Table 3. Whether the gas temperature is high or low, the temperature between the two surfaces is the same, indicating that there is no temperature and oxygen variation within the reacting soot bed. This also indicates that the soot combustion takes place throughout the bed. Recognizing these values at the two surfaces of the soot bed, we can obtain the profiles of temperature and oxygen inside and beyond the soot bed. Fig. 3(a) and (b) represents the results of the one-dimensional simulation with integrated

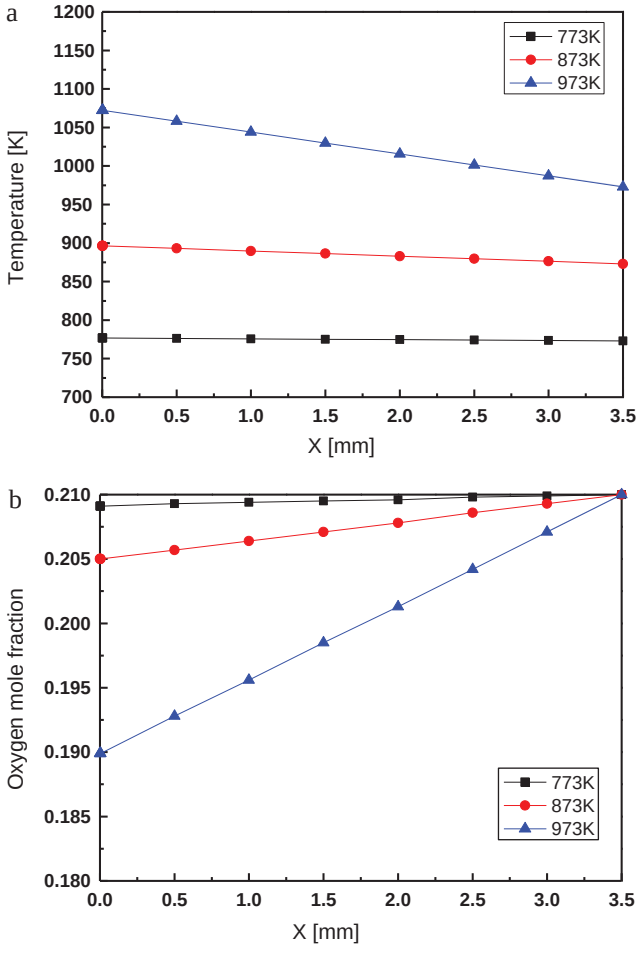

Fig. 3. Results of one-dimensional simulation providing (a) the local variation of temperature and (b) the oxygen content along and beyond the soot bed.

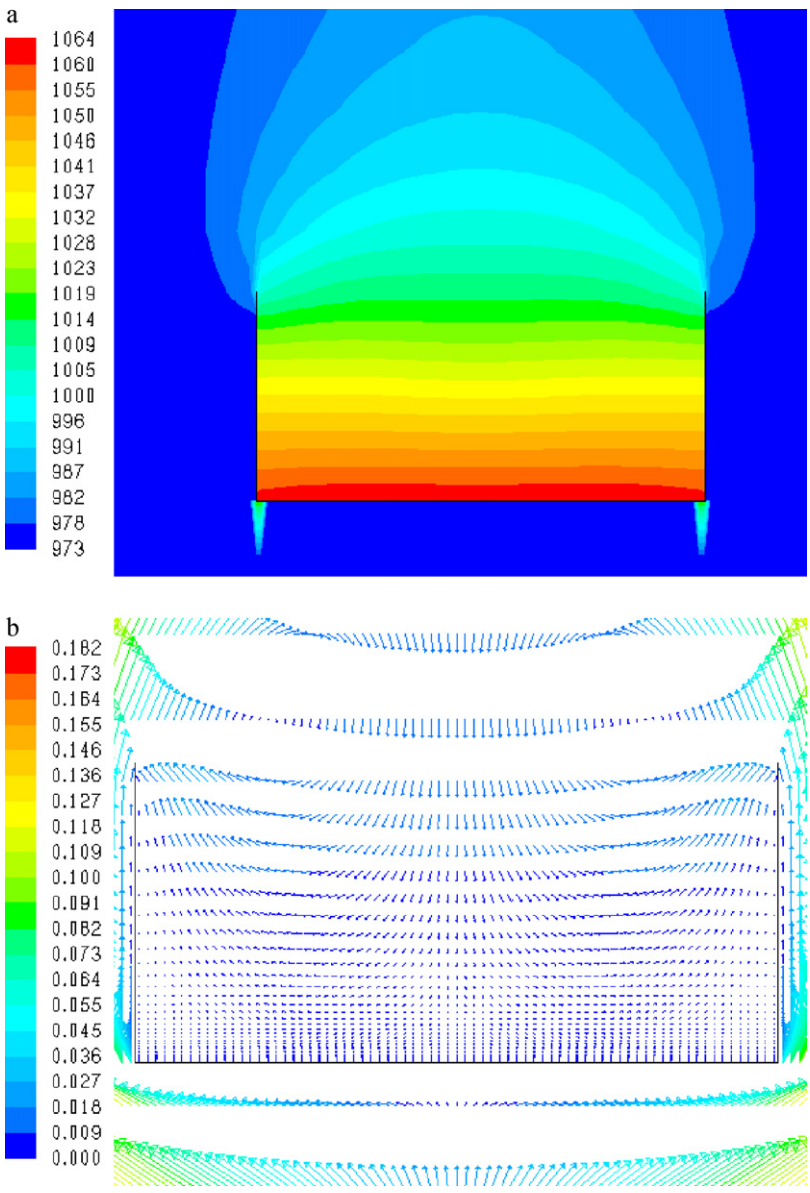

Fig. 4. Results of two-dimensional numerical solution providing (a) the spatial distribution of temperature and (b) velocity around a crucible at the surrounding temperature of 973 K, which are obtained from numerical models where reaction and detailed transport models from advection and diffusion are employed.

models for a local variation of temperature and the molar fraction of the oxygen content within and above the soot bed, respectively.

When the surrounding temperature is considerably low at 773 K, there is no discernable temperature gradient within the particle layer and beyond it. This confirms the validity of the usual assumption that the temperature of the entire packing layer, treated as a lumped mass, remains constant under this condition. As the ambient gas temperature across the crucible increases to 973 K, there is a notable increase in the peak temperature at the top surface when the temperature gradient became relatively steep in the gas phase. This is due to the relatively rigorous exothermal reaction that could produce a considerable amount of mass and generate a relatively high amount of heat. This behavior is well interpreted by a single parameter, heat blowing factor (B_f), which was previously introduced during the discussion of the one-dimensional analysis. Recalling that definition, this factor can be interpreted to be equivalent to the reciprocal of thermal diffusivity, which indicates that the higher this factor is, the less is the heat loss, resulting in a relatively steep temperature gradient along the heat flow direction. When this factor increases by 26 times as predicted with an increase in the gas temperature of 200 K, a relatively steep temperature gradient between the top layer and the top of the wall is prevalent over the crucible since the increase rate of the heat loss effect from the conduction is lesser than the rate of the heat source transferred by the advection. At the relatively high ambient temperature, a higher temperature of the soot bed could provide a faster reaction; this is strongly supported by the observation of the greater depletion of oxygen at the upper surface of the soot bed in Fig. 3(b).

3.2. Numerical solution results

As a more accurate solution, a two-dimensional model of more complexity has been developed for the reacting soot bed beyond which the effect of the vortex flow induced from a positive pressure gradient behind the crucible and the effect of the buoyant flow driven by the product gases produced from a bed reaction may be involved. Figs. 4 and 5 present some results for the spatial distribution of (a) temperature, (b) velocity, (c) oxygen, and (d) CO concentration above the soot bed particularly at the surrounding temperature of 973 K. Again, numerical models and their

simulation include the reaction and the detailed transfer models of heat and oxygen from advection (both from forced and natural free advection) and molecular diffusion. At this condition, the temperature contour in Fig. 4(a) exhibits a nearly one-dimensional variation with respect to the crucible depth. The downward heat advection from a reversed flow and upward heat conduction from a relatively temperature of the bed source at the bottom is well balanced to make the corresponding profile relatively flat particularly in the centerline region where the horizontal variation of temperature is so small that it can be neglected. The velocity contour in Fig. 4(b) confirms that there is indeed the reversed flow pattern where a downward flow occurs near the centerline and then a secondary transverse flow develops toward the two closed sides of the wall because of a buoyant effect from the relatively hot soot bed at the bottom. The initial downward motion was created from a boundary layer separation due to an adverse pressure gradient behind it when the ambient gas flowed over the rectangular crucible.

In contrast, the oxygen contour in Fig. 5(a) is shaped as a bell with a downward curvature rather than a flat shape. This downward direction in which the oxygen is transferred is the opposite to that of the heat diffusion. Furthermore, the oxygen transfer through the advection process is downward since a downward motion of both processes results in a more curved oxygen profile near the centerline as we travels down the bottom. It is important to note that the concentration near the top wall is less than the value (0.21) of the external flow across the crucible. Because of the abovementioned difference in the boundary conditions, a typical analogous relation between oxygen and the heat transfer coefficient may be not applicable to this situation even if the Lewis number, the ratio of the thermal and the mass diffusivities, is equal to one [5]. It is observed that the profile of CO concentration in Fig. 5(b) follows that of O_2 concentration.

These observations imply that the temperature behavior would be predictable readily with the relatively simple one-dimensional model approximation, which does not require the consideration of the two-dimensional flow character. As will be seen in the next comparison section, for this reason, the one-dimensional solution could produce a considerably good agreement with the two-dimensional results in terms of the temperature profile with a minor deviation in the crucible top. However, the prediction of the oxygen and the product gas concentrations may be more difficult with the one-dimensional method probably because of their non-

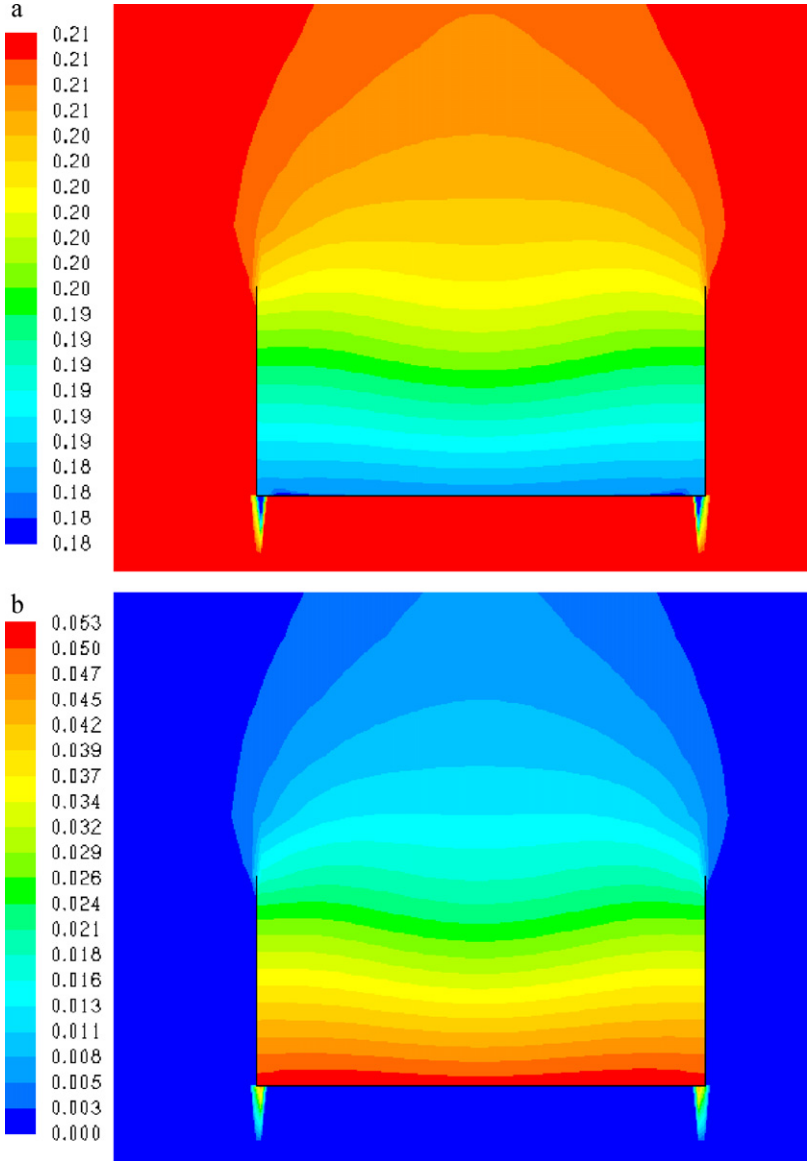

Fig. 5. Results of two-dimensional numerical solution providing (a) oxygen and (b) CO concentration around a crucible at the surrounding temperature of 973 K.

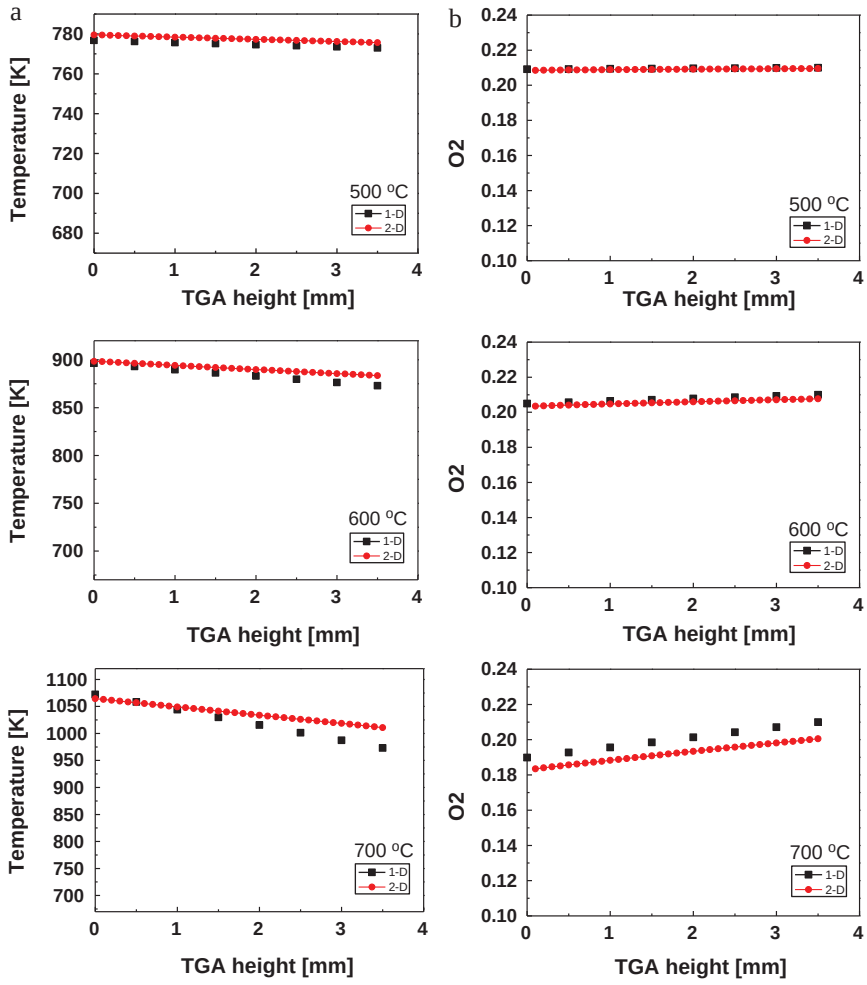

Fig. 6. Comparison of (a) temperatures and (b) oxygen concentrations of gases between one-dimensional analytic and two-dimensional numerical solution under three different temperature conditions of ambient bulk flow: 773, 873, and 973 K.

unidirectional natures. In an ideal situation (in this case) where the amount of soot bed is so moderate as to induce a mild combustion, a free convection effect incurred from the high mass occurring at a high temperature will not be predominant over a forced advection effect. Therefore, the momentum of buoyant flow produced from the former effect in the upward direction is not sufficiently high to push the primary reverse flow developed across the crucible. This situation will arise at a specific instance when the amount of the soot bed is excessively increased and will be evaluated in the subsequent section.

3.3. Comparison of two solutions

In Fig. 6, the gas temperature and the oxygen concentrations are compared in terms of magnitude and the slope in the vertical direction of the crucible for the one-dimensional and two-dimensional simulations. For a fair comparison, an average was taken over the entire cross-sectional area for the two-dimensional results. Overall, both methods would in principle predict the general behavior of a relatively high stream wise gradient with an increase in the ambient gas temperature. In particular, it was found that the differences in the gas temperature between the two solution methods were within the range of 5–10% of the peak temperature for most of the regions around the crucible, which becomes slightly great as the ambient temperature increases. For example, at the top side of the bed, the one-dimensional result shows the peak temperature of 776.8 K at 773 K, 896.3 K at 873 K, and 1072.2 K at 973 K, as listed in Table 3, while the two-dimensional result shows a comparable magnitude. As already described, a relatively large deviation of the two-dimensional result from the one-dimensional result is observed at the crucible top. This is due to the wake motion created from the boundary layer separation caused by an adverse pressure gradient behind a rectangular crucible when the ambient gas flows over it. As the temperature of the ambient bulk gas increases, thereby increasing the pressure gradient, a low temperature is expected at this location because the boundary layer from the wake penetrates further upward. The under predicted result of the one-dimensional analysis may be due to the fact that the cooling from the ambient flow does not offset the heat generated. Because of a similar development of the concentration boundary layer, the concentration at the top crucible is always less than the value of the incoming bulk flow, which decreases with a decrease in the temperature.

The maximum difference in the oxygen content along the crucible lies in the similar magnitude, which is a little greater than that of the temperature since its more non-unidirectional nature would weaken the validity of the one-dimensional prediction. As seen in Fig. 6(b), the wake motion is likely to inhibit the penetration of oxygen transferred through the reversal flow leading to a lower oxygen concentration than the 21% oxygen content of the fresh air at the crucible top. In this region, the one-dimensional solution may not be as accurate as the two-dimensional solution with respect to the representation of this behavior since the one-dimensional analysis uses temperature as an ambient condition. As we reach the bottom,

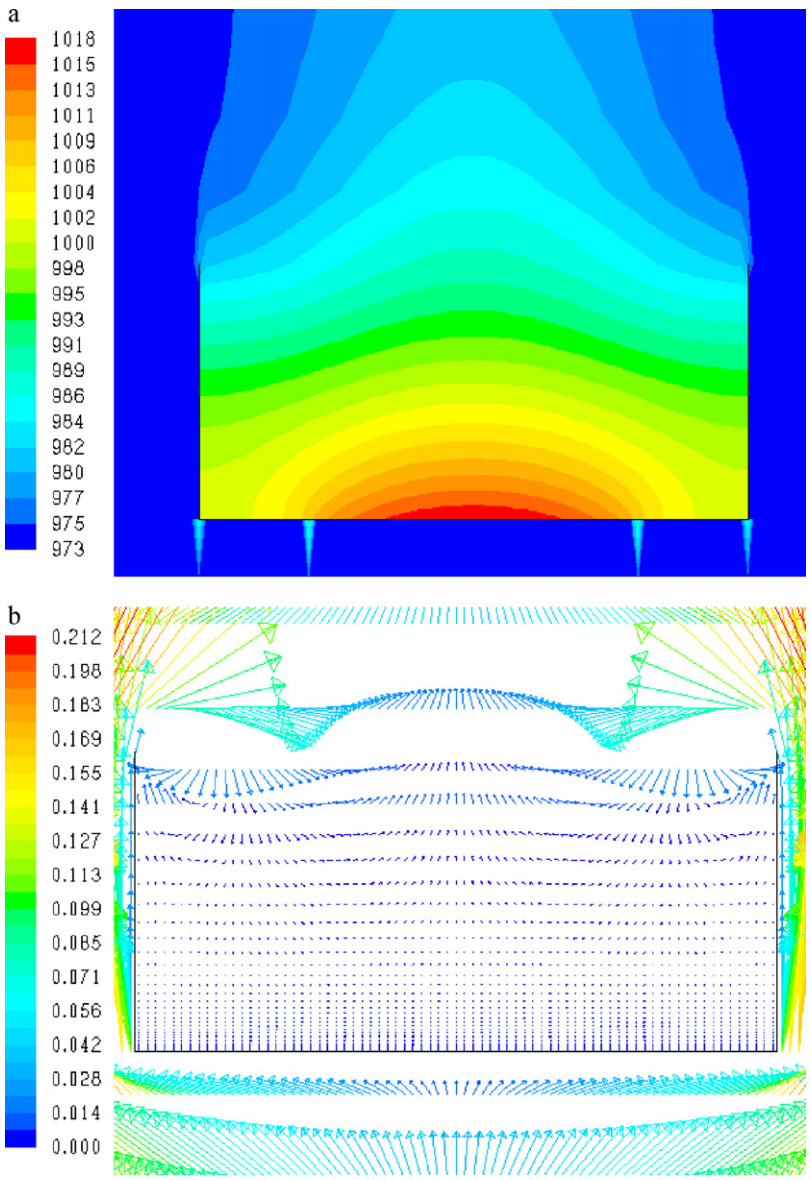

Fig. 7. Combined effects of greater amount of soot bed with uneven deposition on (a) gas temperature and (b) velocity under the elevated temperature condition of ambient flow, i.e., 973 K.

despite the attenuated oxygen transfer from the more-developed boundary layer, the deviation of the two-dimensional result from the one-dimensional result remains unchanged since the downward motion of both the processes are actively involved with the more-curved oxygen profile near the centerline. The understanding of such a non-unidirectional nature of wake motion could lead to the pressing necessity of a two-dimensional numerical simulation at least for an exact prediction of the oxygen and the product gas concentrations.

3.4. Effect of bed configurations

Fig. 7 presents the combined effects of the soot bed weight, and thus the height (10 times greater than that of baseline condition), with an uneven deposition on the increase in the gas temperature and the velocity under one temperature condition of the ambient flow, i.e., 973 K. The soot is placed in a manner such that it fills two-thirds of the crucible width, while ten times the soot amount is loaded with respect to the baseline condition. The situation is used for simulating an unusual condition when the amount of the soot bed is excessively loaded and its deposition is inadvertently distributed. This is evaluated only with the two-dimensional simulation in which the hydrodynamic and geometrical effects are expected to be well described. As compared with the temperature in Fig. 4(a), the temperature profile in Fig. 7(a) becomes even worse toward the top crucible because of the relatively high acceleration of the buoyant flow at the centerline. The velocity profile in Fig. 7(b) shows that the incoming prior downward reversal from the cooler bulk flow is suppressed in a considerably small area near the wall, while the rest of the incoming flow is entrained to the upward buoyant flow of the reacted gases.

As the amount of the soot bed is too excessive to experience any further mild combustion, a free convection effect incurred from the relatively high reaction and mass production becomes more predominant over a forced advection effect (reversal flow) incurred from the boundary layer separation. Therefore, the momentum of the buoyant flow produced from this effect in an upward direction is sufficiently high to push the primary downward flow coming out of the crucible. At this condition, the free boundary layer confined at the two walls because of the buoyancy force is comparable or even

greater than the previous downward motion from the pressure gradient. According to the heat transfer theory [15], this can be easily determined from a comparison of the Grashof number (Gr_{L_∞}) with the square of the Reynolds number ($Re^2_{L_\infty}$). Therefore, this effect is believed to seriously distort the one-dimensional temperature distribution with a flatter shape previously observed under a mild combustion. This implies that the use of the one-dimensional analysis is not sufficient to predict the two-dimensional details of the hydrodynamic flow pattern around the reacting bed in three-sided confined walls.

Such temperature and oxygen distribution resulting from the soot bed configuration is not desirable for the soot oxidation test in the TGA since the reduced amount of oxygen may be supplied to the top of the soot bed because of the attenuated downward motion of the fresh ambient flow. The temperature distribution is unevenly distributed within and beyond the soot bed. As a result, this implies that the small amount of the soot sample should be placed evenly in the crucible.

4. Conclusions

A number of mathematical models have been documented in the literature to describe the rate-controlling combustion processes of the soot bed contained in a confined crucible. However, most of the models have been limited to a separate consideration of a single diffusion process among the two diffusions (heat and oxygen) since a complete coupling of the heat transfer with the mass transfer commonly requires a relatively complicated equation and solution method.

In this study, a new model that accounts for both the transport processes occurring from and into the soot bed is developed. The resultant set of nonlinear equations is solved analytically to obtain the distribution of the temperature and the oxygen content along the surface of the soot bed. A commercially available software package was used for providing a numerical solution that is a more precise representation of the convective and diffusive flows around the crucible and is applicable preferably to soot beds with various geometries.

The comparison of the results shows that the one-dimensional calculation could be applicable for most of the conditions that combine the flow and the soot bed except for the specific conditions of an elevated temperature of ambient gas across the crucible and the high amount of soot bed with an uneven deposition. In particular, as the soot bed lies in the center of the crucible with both sides cleared, the effect of the two-dimensional hydrodynamic attributes such as an upward flow accelerated by the natural convection on the combustion becomes significant.

Acknowledgment

This work is the outcome of a Manpower Development Program for Energy & Resources supported by the Ministry of Knowledge and Economy (MKE).

References

[1] Q. Song, B. He, Q. Yao, Z. Meng, C. Chen, Influence of diffusion on thermogravimetric analysis of carbon black oxidation, Energy Fuels 20 (2006) 1895–1900.
[2] K.K.H. Choy, J.F. Porter, G. Mckay, Film-pore diffusion models-analytic and numerical solutions, Chem. Eng. Sci. 59 (2004) 501–512.
[3] J.H. Song, C.H. Jeon, L.B. Andre, Impacts of oxygen diffusion on the combustion rate of in-bed soot particles, Energy Fuels 24 (2010) 2418–2428.
[4] B.R. Stanmore, P. Gilot, G. Prado, The influence of mass transfer in DTG combustion tests, Thermochim. Acta 240 (1994) 79–89.
[5] R.B. Bird, W.E. Stewart, E.N. Lightfoot, Transport Phenomena, New York, Wiley, 1960.
[6] F. Marcuccilli, P. Gilot, B.R. Stanmore, G. Prado, Experimental and theoretical study of diesel soot reactivity, in: Twenty-fifth Symposium on Combustion, vol. 25, 1994, pp. 619–626.
[7] P. Gilot, A. Brillard, B.R. Stanmore, Geometric effects on mass transfer during thermogravimetric analysis: application to reactivity of diesel soot, Combust. Flame 102 (1995) 471–480.
[8] X.H. Liang, J.A. Kozinski, Numerical modeling of combustion and pyrolysis of cellulosic biomass in thermogravimetric systems, Fuel 79 (2000) 1477–1486.
[9] J.P.A. Neeft, F. Hoornaert, M. Makkee, J.A. Moulijin, The effects of heat and mass transfer in thermogravimetric analysis: a case study towards the catalytic oxidation of soot, Thermochim. Acta 287 (1996) 261–278.
[10] E.J. Bisset, F. Shadman, Thermal regeneration of diesel-particulate monolithic filters, AIChE J. 31 (1985) 753–758.
[11] C.H. Lee, Modeling of single char combustion including CO oxidation in its boundary layer, MS thesis, MIT, 1994.
[12] C.R. Monson, G.J. Germane, A.U. Blackham, L.D. Smoot, Char oxidation at elevated pressures, Combust. Flame 100 (1995) 669–683.
[13] B.R. Stanmore, J.F. Brilhac, P. Gilot, The oxidation of soot: a review of experiments, mechanisms and models, Carbon 39 (2001) 2247–2268.
[14] J.H. Ferrasse, D. Lecomte, Simultaneous heat flow differential calorimetry and thermogravimetry for fast determination of sorption isotherms and heat of sorption in environmental or food engineering, Chem. Eng. Sci. 59 (2004) 1365–1376.
[15] F.P. Incropera, D.P. Dewit, Fundamentals of Heat and Mass Transfer, 4th ed., New York, John Wiley & Sons, 1994.